0031-3998/88/2403-0291$02.00/0
PEDIATRIC RESEARCH

Vol. 24, No. 3, 1988
Printed in U.S.A.

Fluorocarbon Ventilation: Maximal Expiratory Flows and CO_2 Elimination

PETER A. KOEN, MARLA R. WOLFSON, AND THOMAS H. SHAFFER

Temple University School of Medicine, Department of Physiology and Pediatrics, Philadelphia, 19140 and Drexel University, Biomedical Engineering and Science, Philadelphia, Pennsylvania 19104

ABSTRACT. Elimination of CO_2 during liquid ventilation is dependent on flow, diffusion, and the liquid's capacitance for CO_2. Maximum expiratory flow ($\dot{V}_{max}$) and diffusion dead space were measured *in vivo* in 12 young cats during liquid fluorocarbon (FC-80) ventilation to determine the effect of breathing frequency on maximum CO_2 elimination. All animals were maintained (Pa_{O_2} = 255 ± 19 SEM mm Hg, Pa_{CO_2} = 35 ± 1 SEM mm Hg, pH = 7.31 ± 0.01 SEM) within physiologic range during 1–4 h of liquid ventilation. The $\dot{V}_{max}$ in air (26 ± 1 SEM liter/min) and in liquid (1.2 ± 0.2 SEM liter/min) was determined by volume displacement plethysmography. Diffusion dead space (V_{Ddiff}) during liquid ventilation as a ratio of alveolar volume (V_A) was well correlated ($r = 0.84$, $p < 0.005$) with the average time (tav) the liquid was in the lung [$V_{Ddiff}/V_A = 0.89\ e^{(-0.053\ tav)}$]. Alveolar ventilation, CO_2 elimination ($\dot{V}_{CO_2}$), and Pa_{CO_2} were not affected by breathing frequency (f) when tidal volume was adjusted appropriately during steady state liquid ventilation. Predicted maximum CO_2 elimination ($V_{CO_{2max}}$) determined from $\dot{V}_{max}$ and V_{Ddiff} was 24 ml/min at a f of 3–3.5 breaths/min. The maximum was found to be strongly dependent on f with much less dependency on fixed dead space (anatomic plus equipment) and wave shape characteristics. Elimination of CO_2 decreased at low values of f due to inadequate ventilation and at high values of f due to inadequate diffusion time. From a comparison of experimentally determined steady state V_{CO_2} to theoretically predicted $\dot{V}_{CO_{2max}}$, the results demonstrate a f-related functional reserve capacity for CO_2 elimination during liquid ventilation. These findings suggest that by optimizing the liquid ventilatory pattern it should be possible to maintain adequate CO_2 elimination and physiologic Pa_{CO_2} in the presence of pulmonary dysfunction and/or elevated metabolic states. (*Pediatr Res* 24: 291–296, 1988)

Abbreviations

$\dot{V}_{max}$, maximal expiratory flow
V_{Danat}, anatomic dead space
V_A, alveolar volume
$\dot{V}_A$, alveolar ventilation
V_{Ddiff}, diffusion dead space
$V_{Dphysiol}$, physiologic dead space
tav, average time
$\dot{V}_{CO_2}$, carbon dioxide elimination
A-a DO_2, alveolar - arterial oxygen difference
Pa_{O_2}, arterial oxygen tension
PV_{CO_2}, venous carbon dioxide tension
PA_{CO_2}, alveolar carbon dioxide tension
FC-80, fluorocarbon
Pa_{CO_2}, arterial carbon dioxide tension
$P_{E_{CO_2}}$, mixed expired carbon dioxide tension
V(t), net volume
MEFV, maximum expiratory flow volume
V_{Emax}, maximum expiratory volume
T_E, expiratory time
$\dot{V}_{Amax}$, maximum predicted alveolar ventilation
$V_{CO_{2max}}$, maximum predicted carbon dioxide elimination
VC, vital capacity
V_L, lung volume
T_I, inspiratory time
f, frequency

Received May 26, 1987; accepted April 20, 1988.
Correspondence and reprint requests P. A. Koen, Ph.D., c/o T. H. Shaffer, Ph.D., Temple University School of Medicine, Department of Physiology, 3420 N. Broad Street, Philadelphia, PA 19140.
Supported in part by NIH Public Health Grants HL/HD 30525 and 32031.

Several studies have demonstrated that FC-80 ventilation is a feasible alternative to gas ventilation in premature and newborn experimental animals (1–5). Because the air-liquid interface is abolished in the liquid-filled lung, it has been suggested that this elimination of high surface forces could account for effective gas exchange and pulmonary stability. Studies have shown that inflation pressures are reduced (5), lung compliance is increased (1, 2, 6), and PaO_2 and A-a DO_2 are improved (6) in immature lungs after FC-80 ventilation. Although oxygen delivery in these studies has been effective, carbon dioxide removal has been complicated by several factors.

Maintenance of normal arterial carbon dioxide tension during liquid fluorocarbon ventilation is dependent on the rate limiting factors of flow and diffusion (7). The $\dot{V}_{max}$ of liquid from the lung is limited by the wave speed of the fluid (8–10). Furthermore, diffusion of CO_2 into FC-80 is approximately 2500 times slower (7) than diffusion of CO_2 in air and is gradient limited (PV_{CO_2} = 46 mm Hg and PA_{CO_2} = 40 mm Hg). Previous investigators have attempted to quantitate the flow-limiting factor from *in vitro* experiments (7) and the diffusion factor from analytical models (11). The objective of the present study is 2-fold: to quantitate each of the rate limiting factors from *in vivo* animal experiments and to use these results to determine analytically breathing frequencies that will maximize CO_2 elimination during fluorocarbon ventilation.

METHODS

Animal Preparation. Twelve young cats (weight 2.1 ± 0.2 SEM kg) were studied after intraperitoneal anesthesia with pentobarbital sodium (30 mg/kg). The carotid artery was catheterized for blood sampling and a tracheal cannula (4.5 mm OD) was inserted midway along the trachea with its tip positioned proximal to the carina. A baseline set of data was collected during spontaneous air breathing. Each cat was then mechanically hyperventilated

with oxygen for a period of 15 min before the initiation of liquid breathing. This was done to remove nitrogen from the lung, elevate oxygen, and depress carbon dioxide tensions. Succinylcholine chloride (2.0 mg/kg) was administered after the first few minutes of mechanical ventilation to suppress the animal's own respiratory movements. Additional amounts of succinylcholine chloride were administered during the remainder of the study when the animals made spontaneous efforts to breathe.

Liquid ventilation procedure. Liquid ventilation with FC-80 was achieved using a previously described but modified liquid breathing system (4, 12), The apparatus basically consists of bellow pumps and associated valving such that the FC-80 is both pumped into and evacuated from the lungs of the animal. A volume of warmed (37° C), oxygenated liquid, equivalent to the animal's estimated functional residual capacity (30 ml/kg) was then removed from the liquid breathing system. This volume was instilled into the animal's lungs via the tracheostomy tube from a suspended reservoir. Postural and thoracic manipulations were performed to force out any large pockets of oxygen that may have become trapped in the lungs. The animal's tracheal tube was then connected to the liquid breathing system.

A rectal thermocouple (Yellow Springs Instruments, Yellow Springs, OH) was inserted for constant monitoring of the animal's core body temperature. Arterial blood gases as well as fluorocarbon gases were analyzed using a Radiometer electrode system.

Measuring apparatus. Animal weight and flow during liquid breathing were measured by the experimental apparatus shown in Figure 1. The weight platform is supported by three force transducers (Grass model FT01C); electrical signals from which are summed and fed into a polygraph recorder (Grass model 7). With an animal weight of 1 kg the system has a natural frequency of 14 Hz with a damping ratio of 0.019. The drift error after 3½ h is less than 7 g (approximately 4 ml of FC-80).

The volume displacement plethysmograph was constructed based on the Mead (13) design from an infant isolette (33 inch length, 14 inch width, 13 inch height, 0.25 inch thickness) closed at the bottom by a 1-inch Lucite plate and sealed by neoprene O-rings. Air flow was measured with a 400-mesh stainless steel screen pneumotachograph similar to the Lilly (14) design. The pressure drop across the screen was measured with a Statham PM197 differential pressure transducer, with the resulting signal pressure corrected (15) and recorded on the Grass model 7 polygraph. The pneumotachograph was tested and found to have linear pressure flow characteristics up to 30 liter/min.

The undamped natural frequency of the plethysmograph was 6.4 Hz with a damping ratio of 0.7. These values were determined by rapidly pushing air into the plethysmograph. The displacement recording was then analyzed by the method indicated by Fry (16). Volume was measured with a bell-type spirometer. The maximum hysteresis error of the spirometer was less than 3% with tidal volumes less than 100 ml. The undamped natural frequency of the spirometer was 3.7 Hz with a damping ratio of 0.48.

Experimental Procedure. The rate-limiting factors of diffusion and expiratory flow were examined separately in two series of experiments. $V_{Dphysiol}$ was calculated during both air and liquid breathing using the Enghoff (17) modification of the Bohr equation. After the cat was cannulated, $V_{Dphysiol}$ was calculated by recording Pa_{CO_2} and $P_{E_{CO2}}$ as measured with a CO_2 gas analyzer (Godart Type KK) while air breathing. $V_{Dphysiol}$ during air breathing was assumed to be equal to V_{Danat} as occurs in normal animals (18). $V_{Dphysiol}$ space during liquid breathing was similarly calculated with $P_{E_{CO2}}$ being determined from mixed expiratory FC-80. These samples were taken from a port in the liquid breathing system sufficiently downstream (7 feet of 2 inch diameter tubing with three 90° trns) from the animal such that complete mixing of CO_2 had occurred. V_{Ddiff} during liquid breathing (19) which

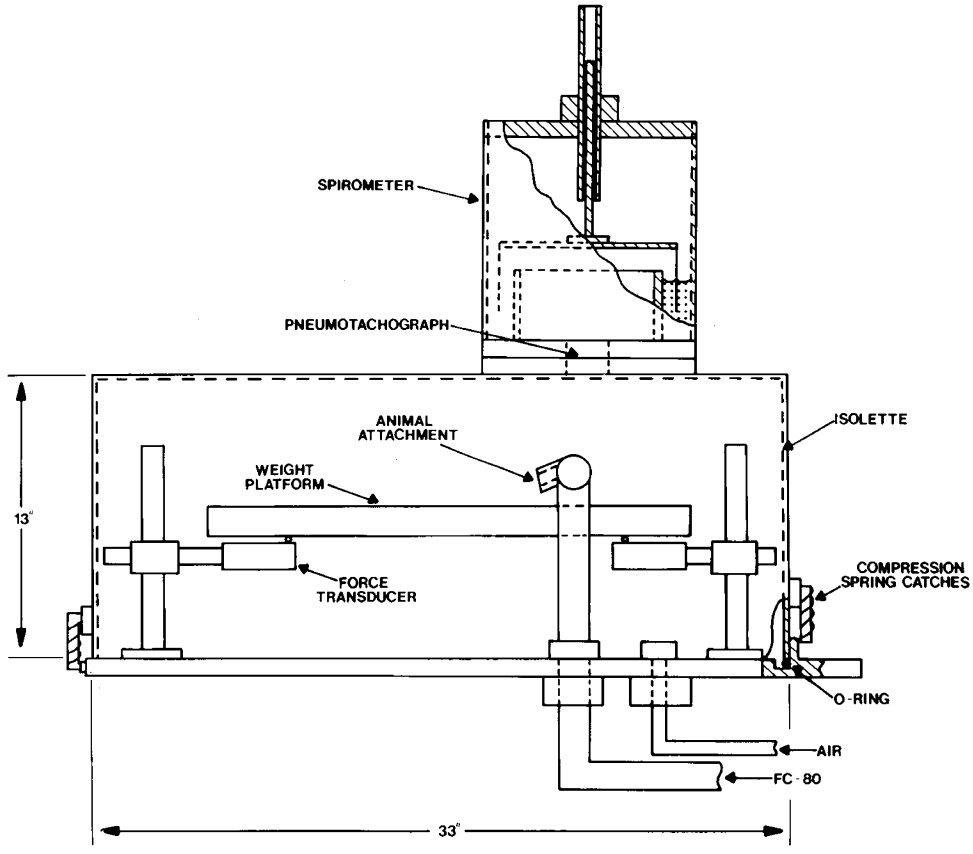

Fig. 1. Schematic of the weight platform and volume displacement plethysmograph. The weight platform is supported by three force transducers: two at the head-end and one at the tail-end. For purposes of illustration only two of the transducers are shown.

results from persisting gradients of gas tension in the lung was obtained by subtracting V_{Danat} determined during gas breathing from $V_{Dphysiol}$, determined during liquid breathing. This calculation assumes that $V_{Dphysiol}$ during gas breathing is attributed entirely to V_{Danat} and that V_{Ddiff} is equal to V_{Dalv} during liquid breathing. Thus, after accounting for equipment and V_{Danat}, all alveolar dead space is assumed to be attributed to diffusion disequilibrium.

During the diffusion experiments V_{Ddiff} was obtained at a minimum of three lung volumes (20–70 ml/kg) and five breathing frequencies (1.5–20 breaths/min) once the animal's blood gases were stabilized at a Pa_{CO_2} less than 45 mm Hg and a pH of more than 7.25. The values of V_{Ddiff} were correlated with the tav that alveolar volume remained in the lung during one breath. Averaged time was computed by integrating the V(t) of liquid exchanged during one breath as shown in equation (1)

$$\text{tav} = \int \frac{V(t)}{Va}\, dt \qquad (1)$$

where Va is alveolar volume and t represents time.

Under steady state conditions, experimental values for effective $\dot{V}_A$ and $\dot{V}CO_2$ were computed as follows:

$$\dot{V}_A = (V_E - V_{Ddiff} - V_{Danat})\, f \qquad (2)$$

and

$$\dot{V}_{CO_2} = Pa_{CO_2}\, \alpha\, CO_2\, (\dot{V}_A) \qquad (3)$$

where there is no CO_2 in the inspired liquid, Pa_{CO_2} is the measured arterial CO_2 tension, α CO_2 is the solubility of CO_2 in fluorocarbon (2.5 ml of CO_2/liter of FC-80/mm Hg), and $\dot{V}_A$ is the alveolar ventilation (ml/min).

Maximum expiratory flow both in air and liquid were determined in the second series of experiments. MEFV curves were obtained in the air after the cat was cannulated, by using the techniques described by Macklem and Mead (20). The lung was inflated to a transpulmonary pressure of 30 cm H_2O by applying a positive pressure to the trachea. A forced deflation was then produced by activating a solenoid valve (fluorocarbon solenoid valve, model DV-3-14A1) which was connected to a 20-liter carboxy previously evacuated to a subatmospheric pressure of 30 cm H_2O (transpulmonary pressure across the lungs and chest wall). The resulting volume and flow signals from the volume displacement plethysmograph were plotted on an X-Y recorder (MFE-model 715M).

The cat was then connected to liquid breathing system and stabilized for a period of 15 min. This was done to insure that any trapped oxygen in the lung was absorbed and therefore would not affect the MEFV curve. $\dot{V}_{max}$ curves in liquid could not be performed in exactly the same way as in air because the maximum tidal volume of the liquid breathing system was less than the vital capacity of the cat's lungs. Therefore, the lungs were first inflated to total lung capacity, as determined from the previous air inflation, and then deflated in three steps. The resulting expired volume and flow signals were recorded on the X-Y recorder. V_{Emax} was computed as function of T_E and $\dot{V}_{max}$ at any given end expiratory volume.

Based on these experiments, the theoretical $\dot{V}_{Amax}$ and carbon dioxide elimination ($\dot{V}_{CO_{2max}}$) at each liquid breathing frequency were computed as follows:

$$\dot{V}_{Amax} = (V_{Emax} - V_{Ddiff} - V_{Danat})\, f \qquad (4)$$

$$\dot{V}_{CO_{2\,max}} = Pa_{CO_2}\, \alpha\, CO_2\, (\dot{V}_{Amax}) \qquad (5)$$

where there is no CO_2 in the inspired liquid, α CO_2 is the solubility of CO_2 in fluorocarbon, assuming a normal Pa_{CO2} of 40 mm Hg.

Differences between gas and liquid breathing variables were assessed by the Student's *t* test for paired samples. Regression analyses were performed by the least squares method. Variability is expressed as mean ± SE.

RESULTS

During the diffusion experiments, the animals were ventilated at several different frequencies (1.5–20 breaths/min) and end expiratory volumes (20–70 ml/kg). Throughout this protocol, tidal volume was adjusted appropriately in order to maintain arterial blood chemistry profiles within physiological range (Pa_{O_2} > 110 mm Hg, 30 mm Hg < Pa_{CO_2} < 45 mm Hg, 7.30 < pH < 7.45). Under these conditions little variability in $\dot{V}_A$ = 47.1 ± 2.7 SE ml/min and $\dot{V}_{CO_2}$ = 4.47 ± 0.40 ml/min was observed.

As shown for one animal in Figure 2, V_{Ddiff}/V_A was typically well correlated with tav ($r = 0.84$; $p < 0.005$) and is described by $\ln(V_{Ddiff}/V_A) = -0.027\text{tav} - 0.24$. Summarized diffusion results for seven animals are shown in Table 1. Based on mean data for all animals, the diffusion dead space during liquid breathing is best represented as $\ln(V_{Ddiff}/V_A) = -0.053\text{tav} - 0.119$. Mathematically, this can also be expressed as $V_{Ddiff}/V_A = 0.89e^{(-0.053\,\text{tav})}$, indicating an exponential decline in V_{Ddiff}/V_A with increasing tav. Regression analysis demonstrated no significant correlation between V_{Ddiff}/V_A and end expiratory volume over the range of data (20–70 ml/kg) analyzed.

MEFV curves for both air and liquid were determined in another group of five animals after a physiologic arterial blood chemistry profile was established. A typical MEFV curve for both air and liquid is shown in Figure 3 and the summarized results from all animals are given in Table 2. As shown in Figure 3, local increases in flow or "bumps" appearing on the liquid MEFV curve, occurred at each of the three steps of the MEFV maneuver in liquid. The $\dot{V}_{max}$ occurring at the beginning of each step exceeds the neighboring areas of the MEFV curve because it takes a definite period of time for the flow to become restricted in the downstream portion of the airway. Furthermore, $\dot{V}_{max}$ during these steps was assured because peak expiratory flow of the liquid system (3.2 liters/min) always exceeded the animals' $\dot{V}_{max}$.

The $\dot{V}_{max}$ of air and liquid for all animals were averaged to construct mean $\dot{V}_{max}$ curves. The $\dot{V}_{max}$ in air (26.0 ± 1 SEM liter/min) for all the animals was significantly more ($p < 0.005$) than in liquid (1.20 ± 0.2 SEM liter/min). The mean $\dot{V}_{max}$ curve in liquid for all animals was correlated with lung volume and expressed as a percentage of the VC. From total lung capacity to 50% of VC, $\dot{V}_{max}$ was essentially constant;

$$\dot{V}_{max} = 1.2 \text{ liter/min} \qquad (6)$$

for 100% VC > V_L > 50% VC.

From 50% of VC to residual volume, $\dot{V}_{max}$ was correlated with V_L ($r = 0.71$; $p < 0.001$) as:

$$\dot{V}_{max} = 0.025\, V_L - 0.03 \text{ liter/min} \qquad (7)$$

for 50% VC > V_L > 0% VC.

V_{Emax} expressed as a function of T_E was determined by integrating equations 6 and 7 using 100% VC and 0% VC as boundary conditions. The results of which are given below:

$$V_{Emax} = 20\, T_E \text{ ml} \qquad (8)$$

for $0 < T_E < 5.3$ s and

$$V_{Emax} = 213 - 106 \exp[-0.19\,(T_E - 5.3)] \text{ ml} \qquad (9)$$

for $T_E > 5.3$ s.

Fifty percent of VC was removed in 5.3 s, whereas 95% was extracted in 16.4 s. T_E that exceed 16.4 s removes only small additional amounts of volume.

Using the theoretical relationships describing $\dot{V}_{Amax}$ and $\dot{V}_{CO_{2max}}$ (equations 4 and 5), experimentally derived regression analysis for V_{Emax} (equation 8 and 9) and diffusion data for V_{Ddiff}/V_A (Table 1), predicted $\dot{V}_{Amax}$ and $\dot{V}_{CO2max}$ were computed and are

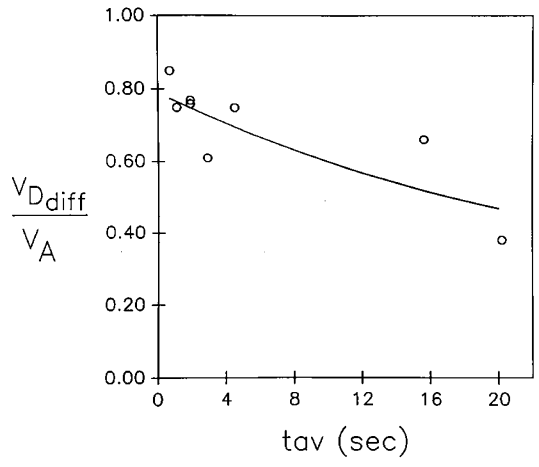

Fig. 2. V_{Ddiff}/V_A as a function of tav in the lung.

Table 1. *Summarized diffusion data**

Cat	Wt (kg)	V_{Danat} (ml)	$\ln (V_{Ddiff}/V_A) = K_1$ tav $+ K_2$ K_1 ($1/s \times 10^{-2}$)	K_2 ($\times 10^{-1}$)
1	2.30	4.50	−2.74	−2.38
2	2.30	6.10	−1.30	−2.14
3	2.20	5.30	−12.04	0.36
4	2.20	6.10	−7.67	−0.02
5	2.60	4.50	−3.20	−1.12
6	1.80	9.20	−2.19	−1.89
7	2.30	5.80	−1.17	−1.12
Mean	2.24	5.93	−5.30	−1.19
±SE	±0.09	±0.60	±1.10	±0.39

* K_1, slope; K_2, intercept.

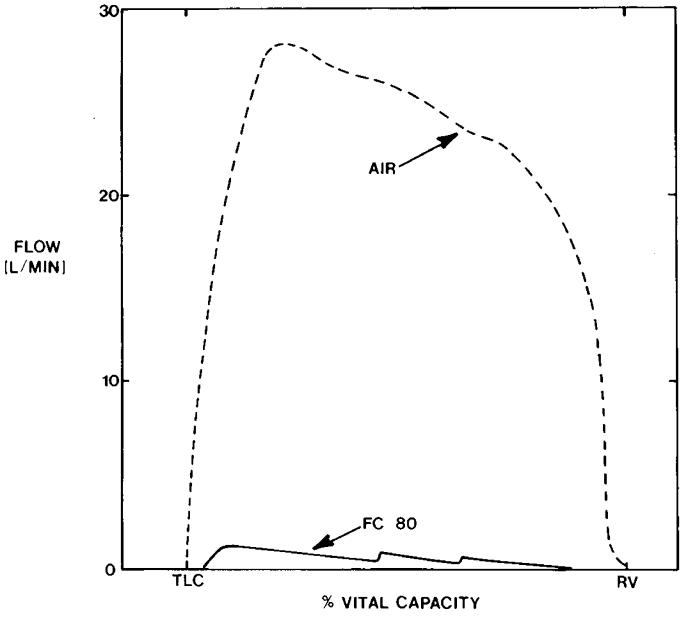

Fig. 3. Typical $\dot{V}_{max}$ curves obtained for both FC-80 and air.

depicted in Figure 4. As shown, peak $\dot{V}_{Amax}$ occurred at approximately 5 breaths/min; whereas peak $\dot{V}_{CO_{2max}}$ was observed between 3–3.5 breaths/min. Both $\dot{V}_{Amax}$ and $\dot{V}_{CO_{2max}}$ were found to decrease at rates above and below these breathing frequencies. It is noteworthy that peak $\dot{V}_{Amax}$ (560 ml/min) and $\dot{V}_{CO_{2max}}$ (24 ml/min) exceed steady state values by approximately 12- and 5-fold, respectively.

Table 2. *Measured $\dot{V}_{max}$ for both air and liquid ventilation**

	Air		Liquid		
Cat	Wt (kg)	$\dot{V}_{max}$ (liter/min)	$\dot{V}_{max}$ (liter/min)	$\dot{V}_{max\,50}$ (liter/min)	$\dot{V}_{max\,25}$ (liter/min)
8	1.7	28	0.88	0.61	0.24
9	2.3	26	1.50	1.50	0.40
10	2.1	28	1.10	1.10	0.36
11	2.4	23	0.80	0.66	0.60
12	2.5	27	1.90	1.90	0.88
Mean	2.2	26	1.20	1.20	0.50
±SEM	0.1	1	0.20	0.30	0.11

* Wt, animal wt; $\dot{V}_{max\,50}$, $\dot{V}_{max}$ at 50% of vital capacity; $\dot{V}_{max\,25}$, $\dot{V}_{max}$ at 25% of vital capacity.

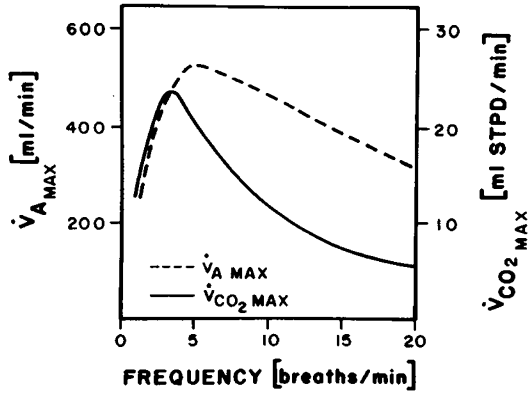

Fig. 4. $\dot{V}_{Amax}$ and $\dot{V}_{CO_{2max}}$ as a function of breathing frequency.

DISCUSSION

In this study we have shown that $\dot{V}_A$ and $\dot{V}_{CO_2}$ during liquid ventilation are determined by the rate limiting factors of diffusion and expiratory flow. We have experimentally determined that diffusional dead space is coupled to breathing f and that $\dot{V}_A$, $\dot{V}_{CO_2}$, and $PaCO_2$ can be maintained constant during steady state ventilation provided tidal volume is adjusted inversely to a change in f. Based on experimentally derived relationships between diffusional dead space, $\dot{V}_{max}$ and f, we have demonstrated that the theoretically predicted maximal $\dot{V}_A$ and $\dot{V}_{CO_2}$ occur between 3–5 breaths/min. In this f range, $\dot{V}_{Amax}$ and $\dot{V}_{CO_2}$ substantially exceed values obtained during steady state ventilation. These findings indicate that f may be a critical determinant of the optimal liquid ventilatory pattern for $\dot{V}_{CO_2}$ during elevated metabolic conditions or pulmonary dysfunction.

Regression analysis of *in vivo* data for the fluorocarbon-filled lung (Table 1) demonstrated a good correlation between V_{Ddiff}/V_A with tav, thus suggesting a decrease in diffusive hinderance with a decrease in breathing frequency. This relationship is presumably explained by the time available for gas exchange within the alveoli. As f decreases, tav increases, thereby allowing more time for CO_2 diffusion across the alveolar capillary membrane and equilibration with the alveolus. Regression analysis demonstrated that this relationship was not affected by end expiratory volume in the range 20–70 ml/kg. In addition, previous studies have demonstrated more uniform blood flow and $\dot{V}/Q$ matching in the fluid-filled lung (1, 21, 22). Therefore, it is unlikely that the apparent alveolar dead space could be due, in part, to nonuniform $\dot{V}/Q$ values in the liquid-filled state.

Although it is difficult to make exact comparisons because of species and equipment differences, previous studies have shown that diffusion disequilibrium does exist during saline and fluorocarbon breathing (19, 23). In comparison to dead space values

in the present study, relatively less diffusion dead space was found in FC-80 ventilated dogs at a respiratory frequency of 2.8 bpm (19) and in human lungs ventilated with saline at a frequency of 2.4 bpm (24). In contrast, Harris *et al.*, (23) recently found dead space ventilation as high as 68% of total ventilation in fluorocarbon ventilated dogs at 3 bpm (calculations were made on mean $P_{E_{CO_2}}$ and Pa_{CO_2} data).

A comparison of the MEFV data shows that there is approximately a 20-fold reduction in liquid flow as compared to air flow. Although *in vivo* data are not available in the literature, *in vitro* studies showed greater reductions in liquid saline flows. Leith and Mead (25) determined MEFV curves from saline-filled dog and rat lungs and found that flows were reduced by a factor of about one-hundred. Hamosh and Luchsinger (26) found a 50- to 100-fold reduction in studies conducted in isolated lungs of young dogs. Furthermore, Schoenfisch and Kylstra (27) found a 40-fold reduction in saline-filled dog lungs and a 50-fold reduction in fluorocarbon-filled lungs.

Density dependence of maximum expiratory flow in humans breathing various air mixtures has been evaluated by previous investigators (29, 30) who found that $\dot{V}_{max}$ for a given medium can be expressed as a function of $\dot{V}_{max}$ for air as

$$\left(\frac{\dot{V}_{medium}}{\dot{V}_{air}}\right)_{max} = \left(\frac{\rho_{medium}}{\rho_{air}}\right)^{-A}$$

where ρ_{medium} is the density of the medium and ρ_{air} is the density of air, and A is an exponent of proportionality. The mean exponent values of A that describe the density dependence found in our experiments ($A = 0.43 \pm 0.05$) were based on the ratio of the density of FC-80 to air. These values were in agreement with previously reported values ($A = 0.41 \pm 0.03$) for different density gases at high lung volumes. In contrast, $\dot{V}_{max}$ at lower volumes may be more dependent on viscosity (μ). Dawson and Elliot (8, 9) have suggested a proportionality of μ^{-1} when viscous effects dominate. Our results showed a proportionality of $\mu^{-0.88}$ at 25% vital capacity. Therefore, $\dot{V}_{max}$ in liquids is probably density dependent at high lung volumes and more viscosity dependent at low lung volumes where smaller airways may be involved.

The time that alveolar volume remains in the lung is determined by the liquid breathing frequency and tidal volume waveforms. Figure 5 illustates an actual and theoretically ideal waveform of a tidal volume at breathing frequency of 5 breaths/min. The actual waveform results from the maximal inspiratory flow capacity (3.2 liter/min) of the liquid breathing system whereas expiratory flow (Fig. 5, *dotted lines*) is dependent on breathing frequency and lung volume. The ideal waveform represents the theoretically maximal inspiratory flow whereas expiratory flows are similar to the actual waveform. This pattern assumes that the inspiratory volume is instantaneously delivered to the lung whereas expiratory flow once again is dependent on breathing frequency and lung volume. To approach this in reality would require extremely high inspiratory flows and concomitant pressures. As shown, both the actual and ideal waveforms reflect variable expiratory:inspiratory timing ratios.

The effect of respiratory timing ratio on $\dot{V}_{Amax}$, tav, and diffusional dead space obtainable with an ideal waveform is depicted in Figure 6. There is a significant increase in $\dot{V}_{Amax}$ with increasing $T_E:T_I$. However, as $T_E:T_I$ increases (Fig. 5, *dotted lines*) the tav that liquid remains in the lung decreases. Less time is available for diffusion; therefore the diffusion process becomes less efficient as evidenced by an increase in V_{Ddiff}/V_A.

Elimination of CO_2 and maintenance of normal Pa_{CO_2} during liquid breathing is dependent on the solubility of CO_2 in the liquid and effective $\dot{V}_A$ (7), which in turn is determined by diffusional processes and expiratory flow limitations. The experimental results from the diffusion protocol demonstate little variability in $\dot{V}_A$, $\dot{V}_{CO_2}$ and Pa_{CO_2} across f. This was accomplished by inversely adjusting the tidal volume to changes in f. Therefore, the increase in diffusional dead space with an increase in f (decrease in tav, Fig. 2) was offset and resulted in maintenance of effective $\dot{V}_A$ and normal Pa_{CO_2}. The ability to maintain normal Pa_{CO_2} during liquid ventilation of young cats is in agreement with findings reported for adult animals (31). Our steady state values of $\dot{V}_{CO_2}$ normalized for body weight were slightly lower than that found by Harris *et al.* (23) during *in vivo* fluorocarbon ventilation in dogs. This may be related to differences in anesthesia, species, control of basal metabolic status, or liquid ventilation techniques and apparatus.

Predicted values for $\dot{V}_{CO_{2max}}$ across f are shown in Figure 7 as a function of waveform. Each curve was determined using the experimentally derived V_{Ddiff}/V_A *versus* tav regression analysis (Table 1) and theoretical relationships describing $\dot{V}_{CO_{2max}}$ (equation 5). Both curves demonstrate that at any given f the predicted $\dot{V}_{CO_{2max}}$ is substantially higher than the experimentally determined $\dot{V}_{CO_2}$ (4.47 ml/min) during steady state ventilation. The ideal waveform (Fig. 7, *dotted line*) is higher at all f because: *1*) V_A increases with the decreasing V_{Danat} and *2*) liquid remains in the

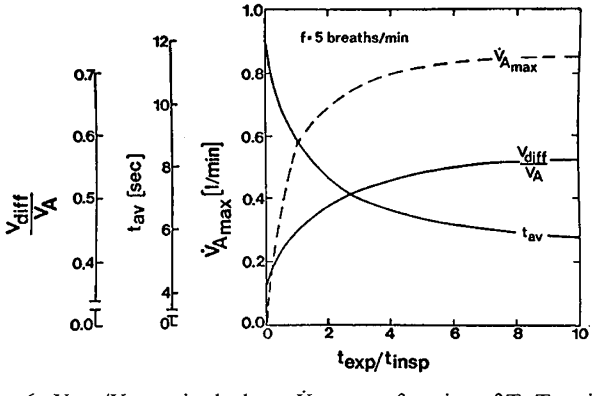

Fig. 6. V_{Ddiff}/V_A, tav in the lung, $\dot{V}_{Amax}$ as a function of $T_E:T_I$ ratios.

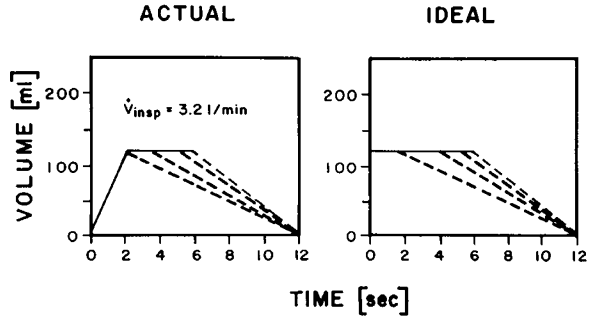

Fig. 5. Schematic representation of an actual and theoretically ideal waveform of a tidal volume at a liquid breathing frequency of 5 breaths/min. $\dot{V}_{insp}$, inspiratory liquid flow; ---, waveforms at different $T_E:T_I$ ratios.

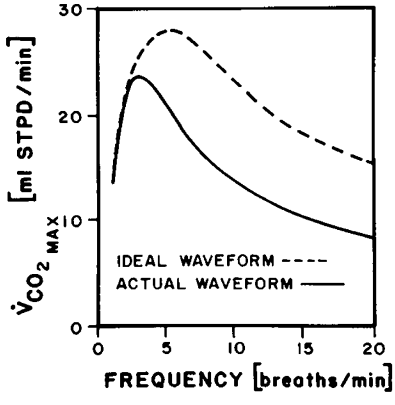

Fig. 7. $\dot{V}_{CO_{2max}}$ as a function of waveform and breathing f.

lung for a longer period of tav due to an increase in T_E:T_I ratio (Figs. 5 and 6). Despite the upward shift of the ideal waveform, the effect on peak $\dot{V}_{CO_{2max}}$ is limited to a net increase of 11%, demonstrating that V_{Danat} and ventilatory waveform have only a small effect on CO_2 elimination during liquid ventilation. The greatest carbon dioxide elimination (peak $\dot{V}_{CO_{2max}}$) is approximately 24 ml/min which represents CO_2 production at about two to three times resting levels. These findings demonstrate a f-related functional reserve capacity for CO_2 elimination during liquid ventilation.

The effect of the relationships between V_{Ddiff}, $\dot{V}_{max}$, and f on CO_2 elimination can be appreciated from Figure 4 wherein the theoretically predicted $\dot{V}_{Amax}$ and $\dot{V}_{CO_{2max}}$ obtainable with an actual waveform is depicted as function of f. In terms of $\dot{V}_{Amax}$, the predicted optimal f occurs at approximately 5 breaths/min where $\dot{V}_{Amax}$ reaches the highest value. $\dot{V}_A$ would have been expected to increase at greater f if tidal volume remained constant. However, as f increases, T_E decreases, the net volume of liquid removed from the lung is reduced, and the resultant tidal volume is decreased. Therefore, $\dot{V}_{Amax}$ is predicted to decrease below peak values at low f due to inadequate ventilation and at high f due to small tidal volumes.

As previously mentioned the predicted optimal f for $\dot{V}_{CO_{2max}}$ occurs between 3 and 3.5 breaths/min. This can be explained as a result of competing factors of alveolar ventilation and diffusion time. As shown in Figure 4, $\dot{V}_{Amax}$ sharply decreases with f less than 5 breaths/min and then gradually declines with f more than this value. However, at slow f, diffusion time increases enabling greater CO_2 exchange; therefore, $\dot{V}_{CO_{2max}}$ decreases at low f due to decreasing alveolar ventilation and at high f due to inadequate diffusion time. The relationships between $\dot{V}_{Amax}$, $\dot{V}_{CO_{2max}}$ and f predicted in this study are similar to those reported by Schoenfisch and Kylstra (7) for *in vitro* liquid ventilated adult dog lungs; however, the f for peak $\dot{V}_{CO_{2max}}$ predicted in their study was more (12 breaths/min) than that found in the present *in vivo* study. This apparent discrepancy may be related to *in vitro versus* our *in vivo* measurement conditions, estimated *versus* our experimentally determined V_{Ddiff}, differences in animal species, or age.

Based on the findings of this study, it should be possible to maintain adequate CO_2 elimination and physiologic Pa_{CO_2} in the presence of pulmonary dysfunction or elevated metabolic states by selecting the appropriate liquid f which minimizes the rate-limiting factors of diffusion and expiratory flow. In conditions of airway obstruction, hyperreactivity, or increased compliance where expiratory flow limitation may be present, slower f would minimize the tendency for airway collapse, resulting in adequate tidal volumes, $\dot{V}_A$, and CO_2 elimination. The effectiveness of slow liquid f in maintaining physiologic Pa_{CO_2} in the presence of highly compliant airways and meconium obstruction has been demonstrated in preterm lambs (1, 4–6). With respect to pathophysiologic conditions such as pulmonary edema which impose diffusional limitations, slow f would provide more time for alveolar and blood gas tensions to approach equilibrium. Using this ventilatory schema, we have observed that normal Pa_{CO_2} can be maintained in adult cats in which pulmonary edema was induced by oleic acid injury (Wolfson MR, Shaffer TH, unpublished observations). *In vivo* evaluation of CO_2 elimination by liquid ventilation during conditions of elevated metabolism has not been performed and requires further study.

Acknowledgments. The authors acknowledge the help, guidance, and support of Drs. G. D. Moskowitz and M. Delivoria-Papadopoulos as well as the technical assistance of E. M. Sivieri.

REFERENCES

1. Shaffer TH, Lowe CA, Bhutani VK, Douglas PR 1984 Liquid ventilation: effects on pulmonary function in distressed meconium-stained lambs. Pediatr Res 18:47–52
2. Rufer R, Spitzer HL 1974 Liquid ventilation in the respiratory distress syndrome. Chest 66:298–199
3. Schwieler GH, Robertson B 1976 Liquid ventilation in immature newborn rabbits. Biol Neonate 29:343–353
4. Shaffer TH, Tran N, Bhutani VK, Sivieri EM 1983 Cardiopulmonary function in very preterm lambs during liquid ventilation. Pediatr Res 17:680–684
5. Shaffer TH, Rubenstein D, Moskowitz GD, Delivoria-Papadopoulos M 1976 Gaseous exchange and acid-base balance in premature lambs during liquid ventilation since birth. Pediatr Res 10:227–231
6. Shaffer TH, Douglas RP, Lowe CA, Bhutani VK 1983 Liquid ventilation: improved gas exchange and lung compliance in preterm lambs. Pediatr Res 17:303–306
7. Schoenfisch WH, Kylstra KA 1973 Maximum expiratory flow and estimated CO_2 elimination in liquid-ventilated dogs lungs. J Appl Physiol 35:117–121
8. Dawson SV, Elliott EA 1977 Wave-speed limitation on expiratory flow—a unifying concept. J Appl Physiol 43:498–515
9. Dawson SV, Elliott EA 1977 Use of the choke point in the prediction of flow limitation in elastic tubes. Fed Proc 32:2765–2770
10. Elliott EA, Dawson SV 1977 Test of wave-speed theory of flow limitation in elastic tubes. J Appl Physiol 43:516–522
11. Kylstra JA, Paganelli CV, Rahn H 1966 Some implications of the dynamics of gas transfer in water breathing dogs. In: De Reuck AVS, Porter R (eds) Ciba—Foundation Symposium, Development of the Lung. Churchill, London, pp 35–58
12. Shaffer TH, Moskowitz GD 1974 Demand-controlled liquid ventilation of the lungs. J Appl Physiol 36:208–213
13. Mead J 1960 Volume displacement plethysmograph for respiratory measurements in human subjects. J Appl Physiol 15:736–740
14. Lilly JC 1954 Flow meter for recording flow of human subjects. In: Methods in Medical Research, vol 2. Yearbook, Chicago, pp 113–121
15. Grimby G, Takishima T, Graham W, Macklem P, Mead J 1968 Frequency-dependence of flow resistance in patients with obstructive lung disease. J Clin Invest 47:1455–1466
16. Fry DF 1960 Physiologic recording by modern instruments with particular reference to pressure recording. Physiol Rev 40:753–788
17. Enghoff H 1938 Volumen Inefficax. Bemerkungen zur frage des schadichen raumes. Ups Lakaref Forh 44:191–218
18. Bouhuys A 1964 Respiratory dead space. In: Fenn WO, Rahn H (eds) Respiration Section Handbook of Physiology, vol 1. Baltimore, Williams & Wilkins Co, pp 699–714
19. Kylstra JA, Paganelli CV, Lanphier EH 1966 Pulmonary gas exchange in dogs ventilated with hyperbarically oxygenated liquid. J Appl Physiol 21:177–184
20. Macklem PT and Mead J 1968 Factors determining maximum expiratory flow in dogs. J Appl Physiol 25:159–169
21. Lowe CA, Shaffer TH 1986 Pulmonary vascular resistance in the fluorocarbon-filled lung. J Appl Physiol 60:154–159
22. West JB, Maloney E, Castle BL 1972 Effect of stratified inequality of blood flow on gas exchange in liquid-filled lungs. J Appl Physiol 32:357–361
23. Harris DJ, Coggin RR, Roby J, Feezor M, Turner G, Bennett PB 1983 Liquid ventilation in dogs; an apparatus for normobaric and hyperbaric studies. J Appl Physiol 54:1141–1148
24. Kylstra JA, Schoenfisch WH, Herrow JM, Blenkarn GD 1973 Gas exchange in saline-filled lungs of man. J Appl Physiol 35:136–142
25. Leith DE, Mead J 1966 Maximum expiratory flow in liquid filled lungs. Fed Proc 25:506
26. Hamosh P, Luchsinger PC 1968 Maximum expiratory flow in isolated liquid-filled lung. J Appl Physiol 25:485–488
27. Schoenfisch WH, Kylstra JA 1971 Maximum expiratory flow from saline and fluorocarbon filled lungs. Physiologist 14:225
28. Lambert RK, Wilson TA, Hyatt RE, Rodarte JR 1982 A computational model for expiratory flow. J Appl Physiol 52:44–56
29. Staats BA, Wilson TA, Laifook SJ, Rodarte JR, Hyatt RE 1980 Viscosity and density dependence during maximal flow in man. J Appl Physiol 38:313–319
30. Wood LDH, Bryan AC 1969 Effect of increased ambient pressure on flow-volume curve of the lung. J Appl Physiol 27:4–8
31. Sass DJ, Ritman EL, Caskey RE, Banchero N, Wood EH 1972 Liquid breathing: prevention of pulmonary arterial-venous shunting during acceleration. J Appl Physiol 32:451–455